UCRL-20303

c.2

ATOM PROBE FIELD ION MICROSCOPE

Kaj Gunnar Stolt
(M.S. Thesis)

AEC Contract No. W-7405-eng-48

UCRL-20303

LAWRENCE RADIATION LABORATORY
UNIVERSITY of CALIFORNIA BERKELEY

DISCLAIMER

ATOM PROBE FIELD ION MICROSCOPE

Contents

ATOM PROBE FIELD ION MICROSCOPE

Kaj Gunnar Stolt

Inorganic Materials Research Division, Lawrence Radiation Laboratory
Department of Materials Science and Engineering, College of Engineering
University of California, Berkeley, California

ABSTRACT

The design and performance of an atom probe field ion microscope is described. This instrument consists of a normal field ion microscope connected to a time of flight spectrometer. The microscope is a bakeable all metal system with a capability of reaching a pressure of 10^{-9} torr. A dynamical supply of the imaging gas is utilized to facilitate the operation of the probe. Cold helium gas pumped from a liquid helium dewar is used for cooling the tip. The specimen holder provides excellent electrical shielding of the tip region where the acceleration of the field evaporated ions takes place, and also cools this region which is a favorable feature. The specimen can be centered to within ± 0.2 mm of the axis of the drift tube and is rotatable through its tip by ± 45 degrees vertically and ± 90 degrees horizontally. The cooling of the tip is not effective enough and at present the tip temperature can be brought down to only 40°K. Another shortcoming of the specimen holder is its inability to withstand higher voltages than 15-20 kV.

The instrumentation of the atom probe is presented and it is shown that with the present instruments the mass resolution is limited to about $m/\Delta m = 100$. This is illustrated by a mass analysis of tungsten.

A method of calibrating the atom probe is described and the factors that limit the resolving power of the instrument are briefly discussed. It is shown that improving the instrumentation could improve the resolution by about a factor of 2.

was obtained in this manner.[4] About five years later it was realized that cooling the specimen would improve the resolution through accomodation of the image gas to the tip temperature,[5,6] and at about the same time field evaporation was discovered.[7] Field evaporation refers to the evaporation of atoms from the surface of the metal tip under the effect of the electric field, and is of the utmost importance to field ion microscopy since without it the necessary final shaping of the tip to an atomically smooth endform would not be possible. With these two contributions the fundamental ingredients of modern field ion microscopy were known. Further progress was brought about mainly by the introduction of various in situ treatments of the specimen, application of field ion microscopy to metallurgical research, and by refinement of the theory (for a review and extensive bibliography see Ref. 1). With the collection of more data in the form of field ion images it became obvious that a serious shortcoming of the FIM was its inability to identify the atomic species of the surface atoms responsible for the image dots. An identification of the chemical nature of surface atoms would have obvious practical applications, e.g. in the study of short range order in alloys, the nature of precipitates, adsorption of atoms on the surface, etc., and could also shed light on fundamental problems pertaining to the imaging properties of different atomic species. In 1968 a device with the potential ability of identifying any one atom on the field ion tip chosen by the discretion of the experimenter was presented by Müller.[8] A short time later a similar instrument was constructed by Brenner and McKinney.[9] This instrument was given the name atom probe FIM.

The atom probe FIM is a combination of a normal field ion microscope

and a mass spectrometer in the form of a time of flight analyzer. The specimen is mounted in the microscope and imaged in the usual way. The specimen holder allows for rotation of the specimen about two different axes so that any one dot in the image, and hence the corresponding surface atom, can be positioned over a probe hole in the center of the screen. After removal of the imaging gas from the microscope an atom thus positioned is made to fly off the tip and through the probe hole by application of a positive voltage pulse to the specimen, which causes the surface atoms to field evaporate. In the process of field evaporation the atom loses one or several of its electrons, i.e. it leaves the surface as an ion. The ion is collected with a detector at the far end of a drift tube behind the screen. By having the evaporation pulse start and the detector signal stop a timer, the flight time of the ion is measured. Fig. 1 shows the instrument schematically.

If the duration of the evaporation pulse is long enough so that the ion has travelled into a region of essentially ground potential when the pulse falls off, the kinetic energy of the ion is given by the sum of the constant image voltage and the pulse voltage:

$$\frac{1}{2} mv^2 = ne\,(V_{dc} + V_{pulse}). \qquad (1.1)$$

n is an integer indicating the degree of ionization, e is the electron charge and m and v the mass and velocity of the ion. Since the electric potential falls off very rapidly with distance from the tip, (as r_t/r, where r_t is the tip radius and r the radial distance), the ion will reach its final velocity in a distance that is negligible compared to the length of the flight path. The ion may hence be considered to move with a constant velocity from tip to detector and the time of flight is

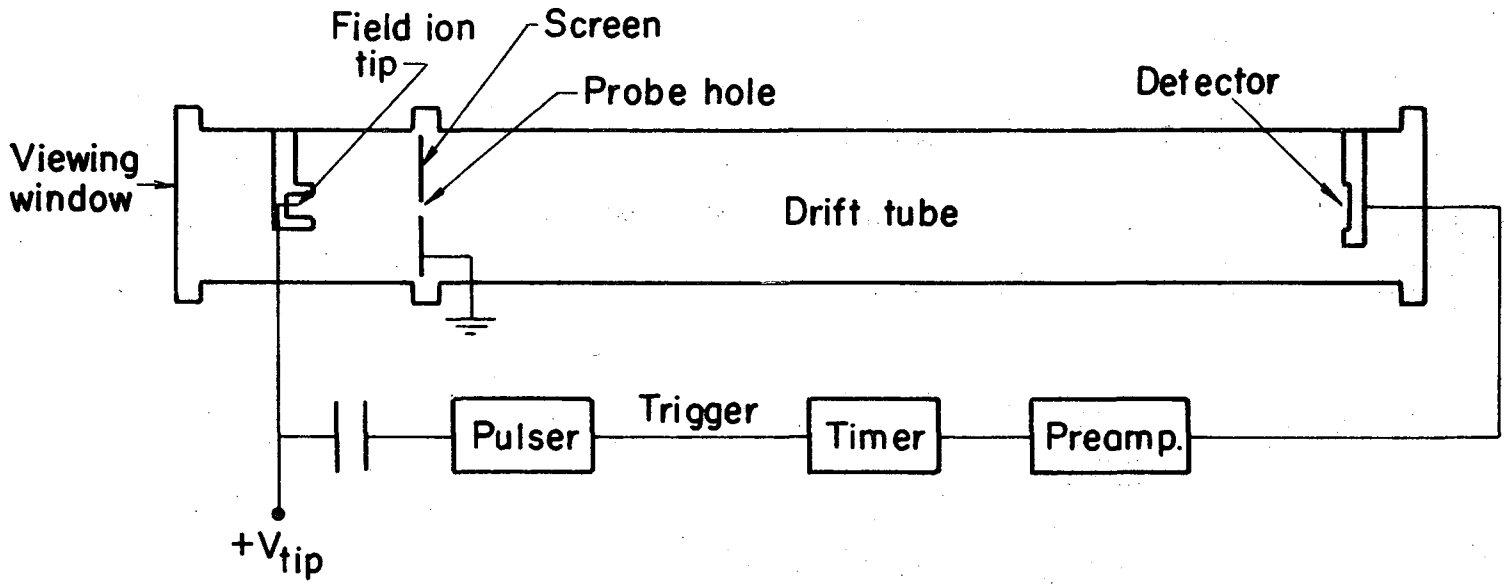

XBL 709-6483

Fig. 1. The atom probe field ion microscope.

given by

$$t = \ell/v, \tag{1.2}$$

where ℓ is the tip to detector distance. Elimination of v from Eqs. (1.1) and (1.2) leads to the following expression for the mass to charge ratio of the ion:

$$\frac{m}{n} = \frac{2e\ (V_{dc} + V_{pulse})}{\ell^2}\ t^2 \tag{1.3}$$

A measurement of t thus yields m/n which identifies the ion.

In the foregoing the assumption was made that a positive voltage pulse was applied to the tip to effect the field evaporation. A negative voltage pulse applied to a ring just in front of the field ion tip would have the same effect, and this mode of operation was in fact used in the atom probe designed by Brenner and McKinney.[9] This offers the advantage that the pulse voltage will not appear in the kinetic energy of the ion. If the pulse is of long enough duration the ion will return to ground potential outside the ring before the pulse falls off, in which case the ion will have picked up a net energy corresponding to only the tip voltage (V_{dc}).

When the construction of the instrument to be described was being planned only the two atom probes mentioned above were reported in the literature. No details of the mechanical design of the Brenner-McKinney instrument were known except that it was an all metal construction. Müller's instrument was based on a glass microscope with a greased ball joint providing the necessary rotation of the tip.

The goal set for the present instrument was in the first place excellent vacuum performance. This calls for an all metal system and

also requires that the specimen be tilted by means of a vacuum tight feed-through manipulator. Versatility of application was considered important and hence additional ports for vacuum deposition of atoms on the tip, or for ion or electron bombardment etc. were provided. Photography of the image before and after the field evaporation event is sometimes important. This feature is realized in the present instrument.

At an early stage of the development of the present instrument the idea evolved that the mass resolution of the atom probe could be improved by increasing the time of flight. If a longer time can be measured with the same absolute accuracy then, obviously, the relative accuracy will be higher. There are two ways to increase the time of flight. One, which is now being pursued by Müller,[10] is to use a longer drift tube. The other is to slow down the ion for part of the drift space. The latter, which can be brought about by the assembly shown in Fig. 2, seemed to be promising at the time, and it was decided to build an instrument according to Fig. 2. It will be noticed that removal of the drift tube and voltage plates transforms this instrument into a conventional atom probe.

Since the decelerating voltage is deflecting a focusing electrostatic lens had to be designed for the space between $z = 0$ and $z = a$ of Fig. 2. Due to extensive delays in the machining of the lens the development of the atom probe proceeded, to begin with, on the line of a conventional probe.

Originally the plan was to design an instrument utilizing the pulsed-ring mode of Brenner and McKinney mentioned above. A considerable amount of time was spent on designing a satisfactory assembly for the field ion tip-voltage ring combination with separate voltage lines for

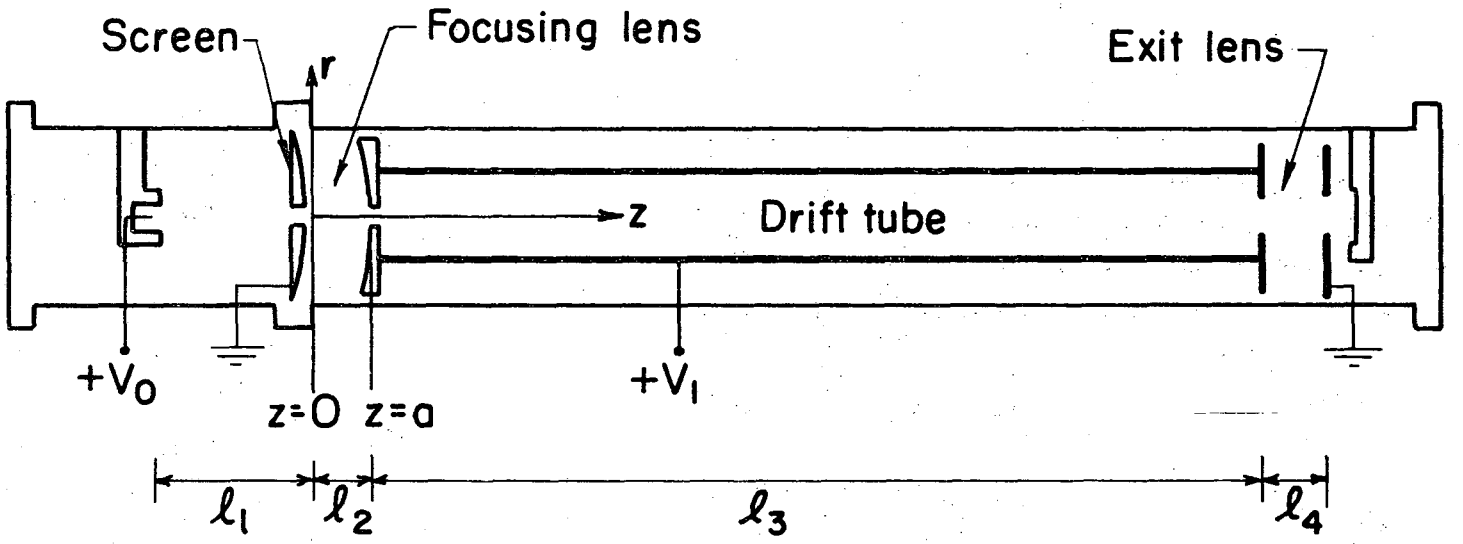

XBL 709-6486

Fig. 2. The atom probe with a retarding electrode system.

the image and pulse voltages. A special 51 ohm pulse line was even built for distortionfree transmission of the pulse. The construction of such an assembly turned out to be very difficult, however, and this mode of operation was finally abandoned in favor of the one where the pulse is applied directly to the tip. Even so the specimen holder turned out to be the overwhelming design problem.

In the following the construction and instrumentation of the atom probe is presented, and its operation is briefly described. The mass resolution of the atom probe, is then discussed and a method for calibrating the atom probe is presented. As an example the results of an actual calibration are given. Finally the design of the electrostatic lens system is presented, and the possible advantages of its use are analyzed.

2. CONSTRUCTION

The design problems of the atom probe FIM can for clarity be divided into four groups: vacuum system, cooling of the specimen, mechanical motion of the specimen, and electrical insulation. While the design of the vacuum system can proceed without regard to the other three items, the cooling, the motion and the electrical insulation must in practice be treated together. Therefore one major problem is the design of a specimen holder that allows for mechanical rotation of the field ion tip, while still, at the same time, maintaining good thermal contact with and electrical insulation from the cryostat.

2.1. The Vacuum System

Field ion microscopy requires, even in its crudest applications, a vacuum level in the 10^{-6} - 10^{-7} torr region. For more sensitive work pressures below 10^{-9} torr may be necessary. Vacuum technology today is well advanced to meet such requirements in a bakeable all metal system. A drawback at present is the excessive pumping time after each change of specimen in order to recover the ultra high vacuum which makes use of the instrument very time consuming.

Figure 3 shows a schematic drawing of the vacuum system. The microscope chamber is a 22 cm long, 6" diameter stainless steel tube to which is connected the atom probe drift tube of the same diameter and 1 m in length. The total volume of this system is about 60 liters. Pumping out is started by the nitrogen pressure jet which in one minute reduces the pressure to the 100 torr region. From there on the liquid nitrogen cooled molecular sieve traps bring the pressure down to 5 microns in half an hour, at which pressure the mechanical pump-diffusion pump

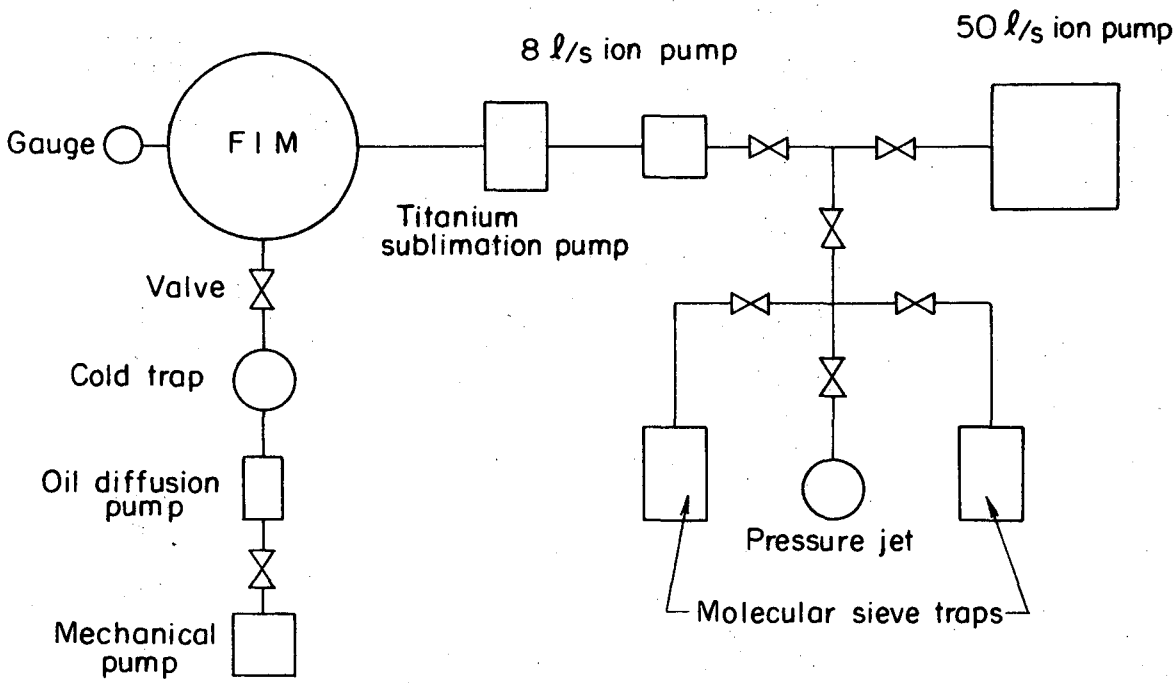

Fig. 3. The vacuum system.

branch takes over the pumping reducing the pressure to the 10^{-5} torr region almost immediately. A light bake-out is performed in this stage for about 3 hours. The temperature must be kept fairly low due to the ion detector that can stand only 140 °C. After cool down pumping is continued with the sublimation pump together with either of the ion pumps. In this manner a pressure below 10^{-8} torr can be attained in about one day.

2.2. The Cryostat

Reasonable field ion images can be produced with liquid nitrogen cooling of the tip, but full exploitation of the potentialities of the field ion microscope requires lower temperatures. The main advantage of a lower temperature is the increased image brightness, but also the resolution is improved by cooling. A helium ion image e.g. is twice as bright at 21°K as at 78°K while the resolution improves about 25-30% by cooling to the lower temperature.[1]

Liquid helium was chosen as the coolant mainly because it is readily available at our laboratory. Liquid hydrogen is commonly used in field ion microscopy, but was ruled out here as too hazardous. It was found most convenient to design a cryostat that does not accumulate liquid helium in a dewar but rather is cooled by a continuous flow of boiled off helium gas. This allows for faster warming up after an experiment, while still maintaining the temperature low enough. The cryostat is simply a stainless steel tube surrounded by a vacuum mantle as sketched in Fig. 4. The cryostat is mounted on top of a stainless steel bellows as illustrated in Fig. 5. By tightening or loosening the bolts supporting the bellows the specimen holder that is mounted on the end of the cold

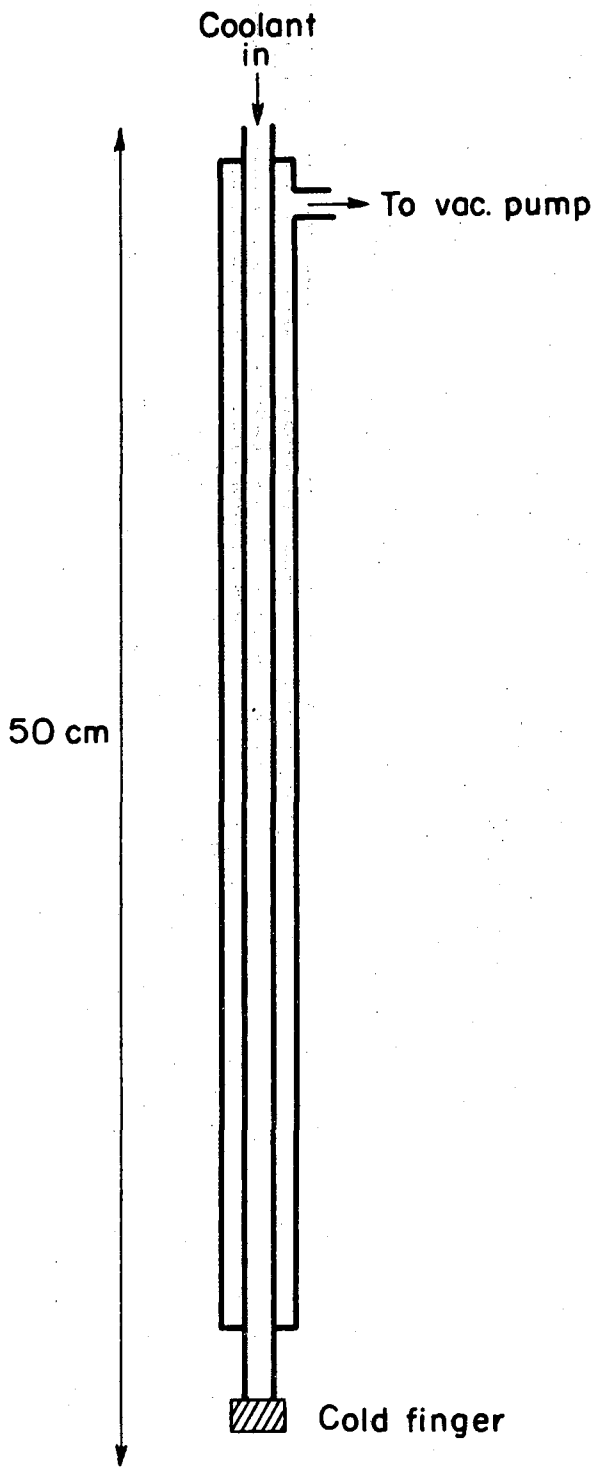

XBL 709-6487

Fig. 4. The cryostat.

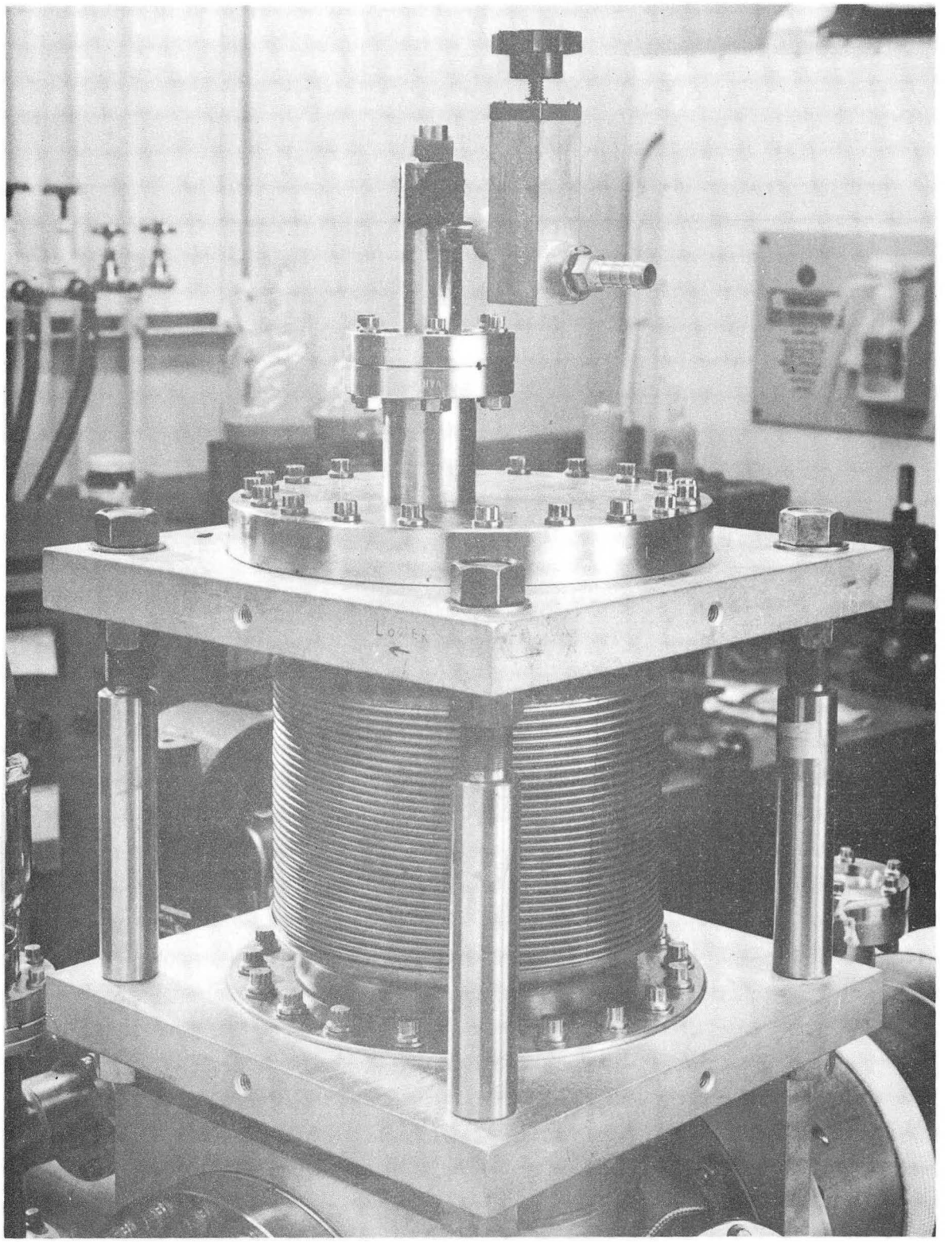

XBB709-3969

Fig. 5. Bellows for tilting the cryostat.

finger can be moved horizontally and vertically. This allows for positioning of the specimen tip on the line connecting the probe hole and the center of the sensitive area of the detector.

2.3. The Specimen Holder

The specimen holder consists of two parts: a drum that carries the specimen and a hollow block in which the drum rotates. Both are made of high purity alumina which offers electrical insulation and a fairly high thermal conductivity. The drum and the block are precision machined for perfect fit. A cross section of the drum is shown in Fig. 6a. The copper plug is tightly pressed into the drum and connected to the high voltage by a wire through the axis of the drum, Fig. 6b. The specimen is spotwelded to a spring of tungsten wire, Fig. 6c, which is pushed into the two holes in the copper block, to a depth such that the tip of the specimen is exactly on the axis of the drum. By rotating the drum the field ion image can be moved up and down on the screen. The purpose of the grounded steel ring and aluminum plate is to shield the region surrounding the specimen from stray electric fields. The drum can be removed from the block by removing one of the sidewalls of the block, Fig. 7. Figure 8 shows how the specimen holder is attached to the cold finger. The alumina block is tightly screwed into a coppersleeve connected to the cold finger by a sliding pressure contact. Thus the whole specimen holder is rotatable about a vertical axis passing through the center of the drum. The tip of the specimen should also be on this axis. This rotation about the vertical axis moves the image sideways and hence any part of the image can be placed over the probe hole as required. Since the specimen rotates around its tip the position of the tip is fixed

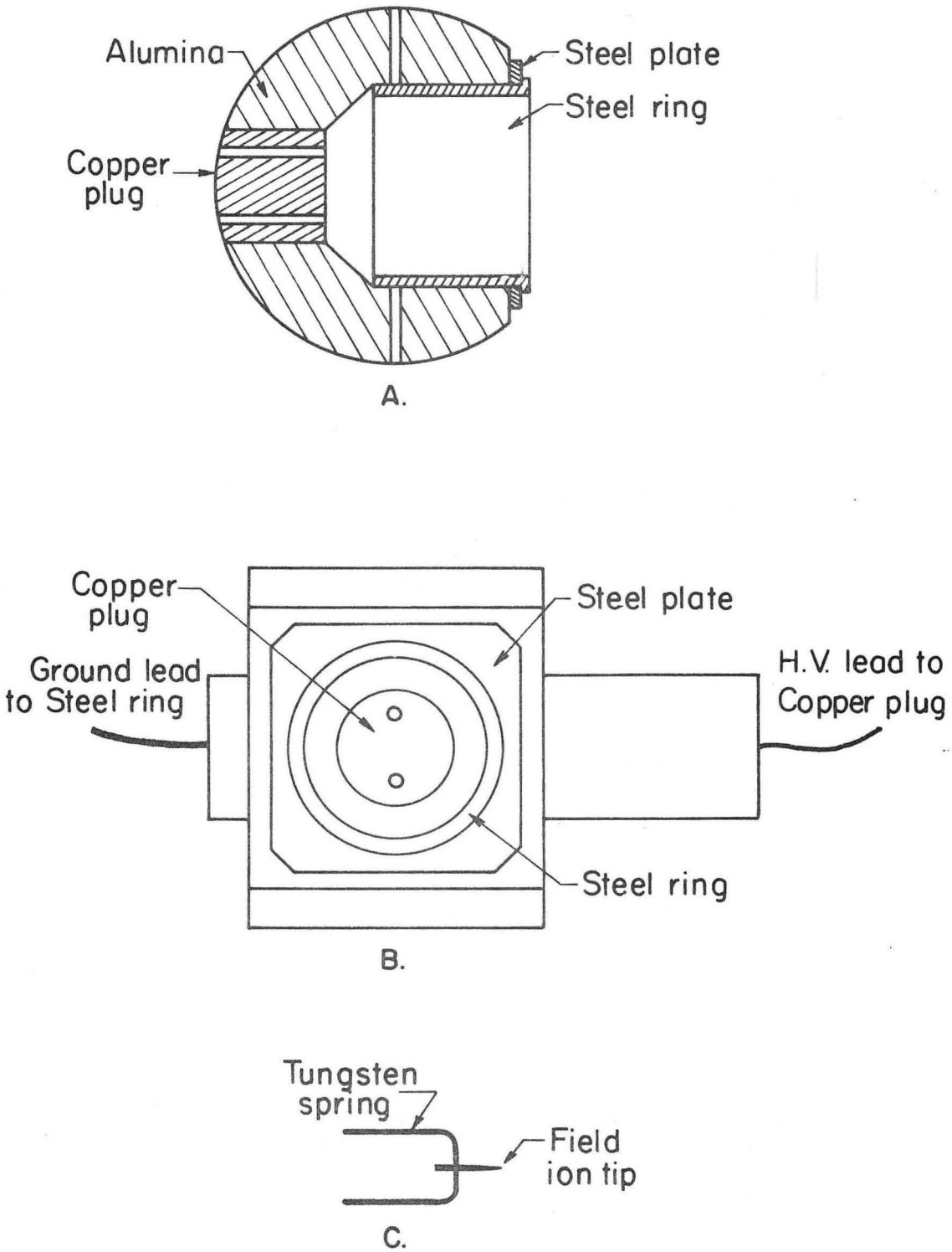

Fig. 6. The specimen mount.

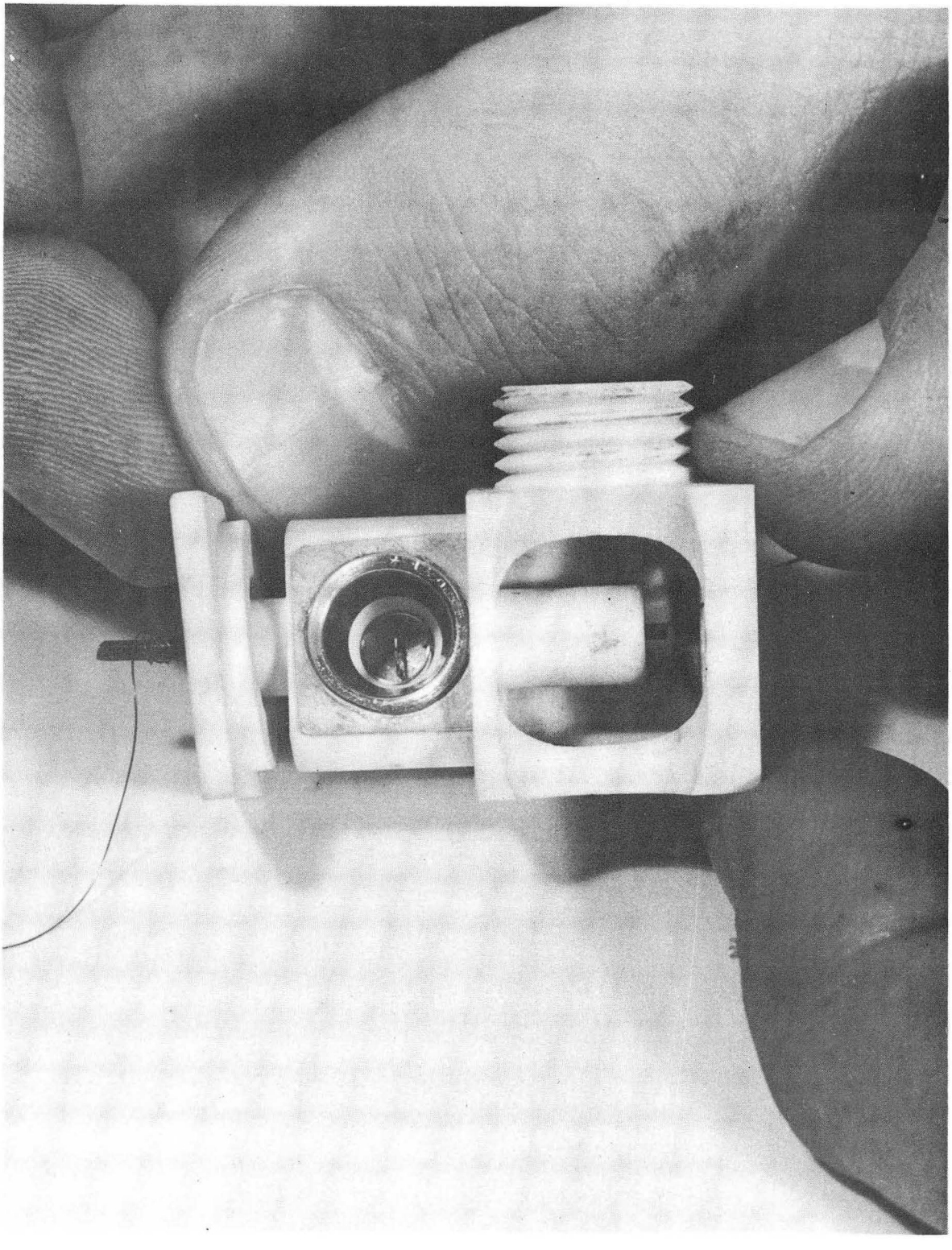

XBB709-3971

Fig. 7. Assembling of the specimen holder.

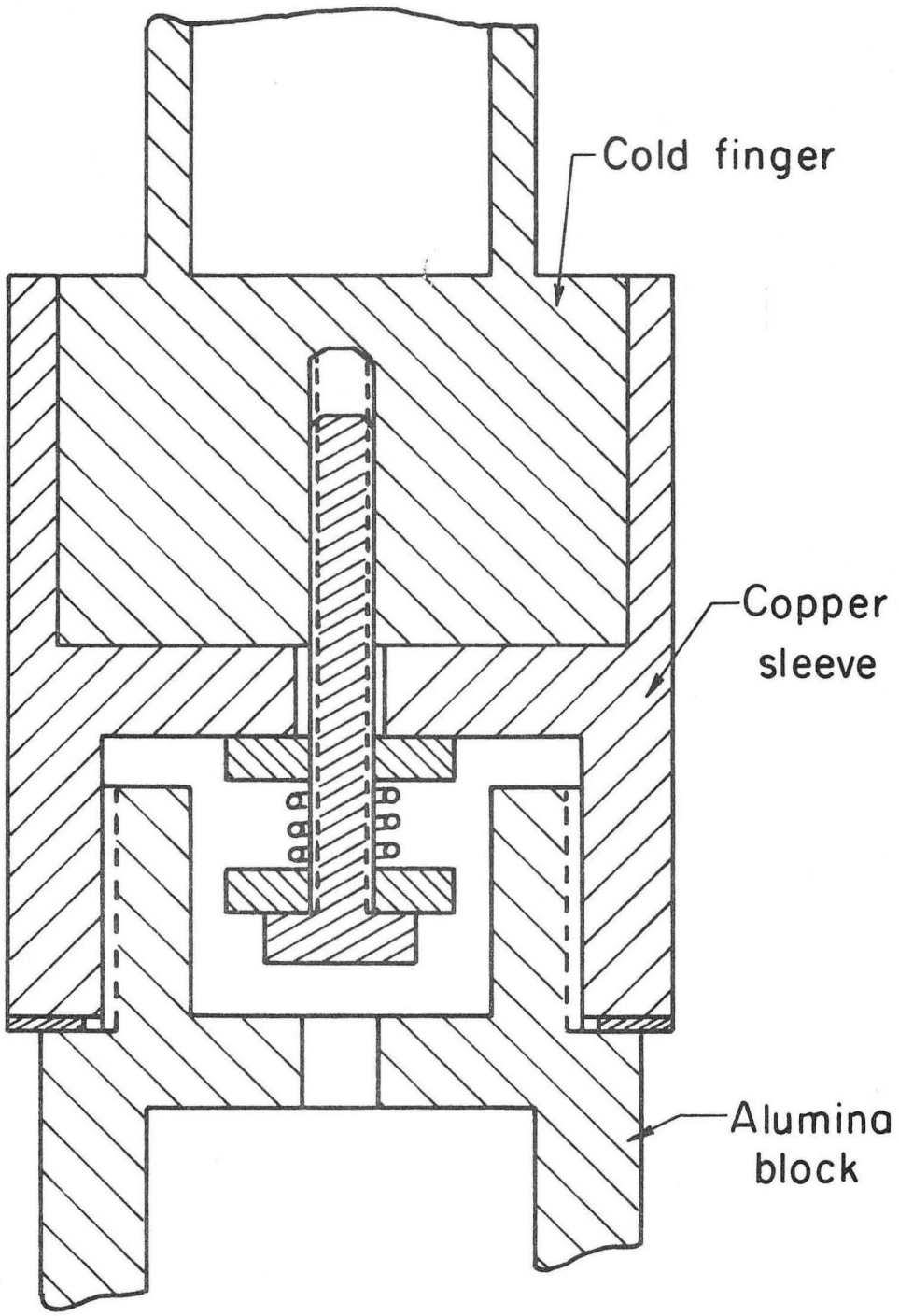

XBL 709-6482

Fig. 8. Mounting of the specimen holder on the cold finger.

during rotation and hence alignment is preserved when the image is moved.

To improve the thermal contact the copper sleeve is pressed against the cold finger and the drum against the block by means of external springs in the manner illustrated in Fig. 9. Still the cooling of the specimen which has been achieved by this design is only, at best, acceptable. The lowest tip temperature is about 40°K, and can be maintained with a liquid helium consumption of 2-3 ℓ/h. The two sets of sliding interfaces present too much hindrance to heat flow to allow more effective cooling. A favorable feature of the design is the fact that the space surrounding the specimen is well cooled.

Electrically the specimen is very well shielded from external fields inside the stainless steel cylinder. However, at a voltage level of about 15 kV electrical breakdown occurs somewhere in the specimen holder. By covering the alumina block with aluminum foil the breakdown voltage can be raised to 20 kV but this is still too low for some applications, and improvements are called for.

The mechanical motion for rotating the specimen is provided by a rotary motion-linear motion bellows combination, which transfers motion to a vertical rod inside the microscope. This assembly is shown in Fig. 10. The rotation of the rod rotates the tip holder about its vertical axis, whereas the vertical linear motion rotates the drum, by the mechanisms in Fig. 11. The specimen manipulator performs quite satisfactorily, and every part of the image can easily be brought over the probe hole.

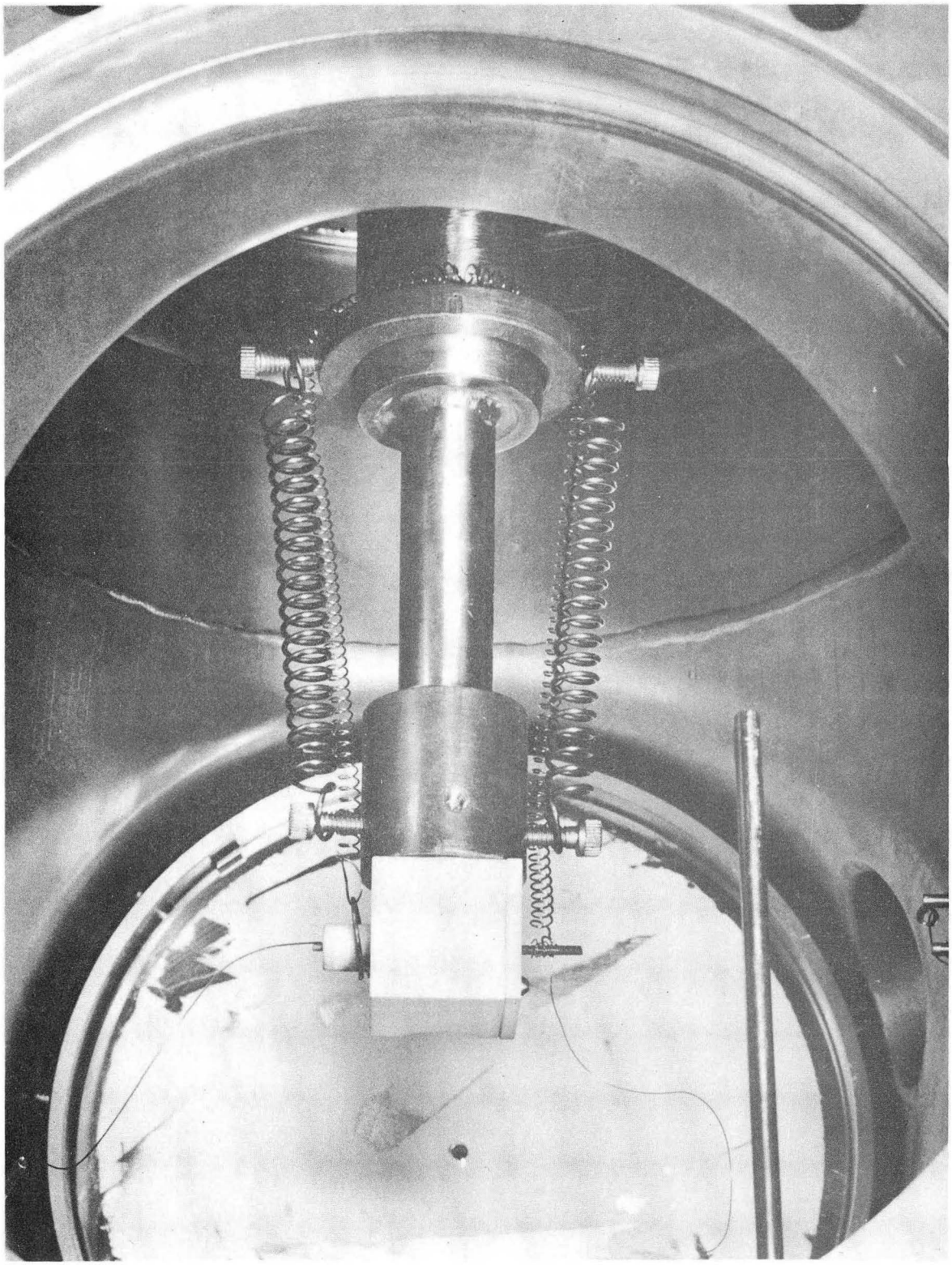

XBB709-3970

Fig. 9. Springs for enhancement of the thermal contact between the specimen holder and the cold finger.

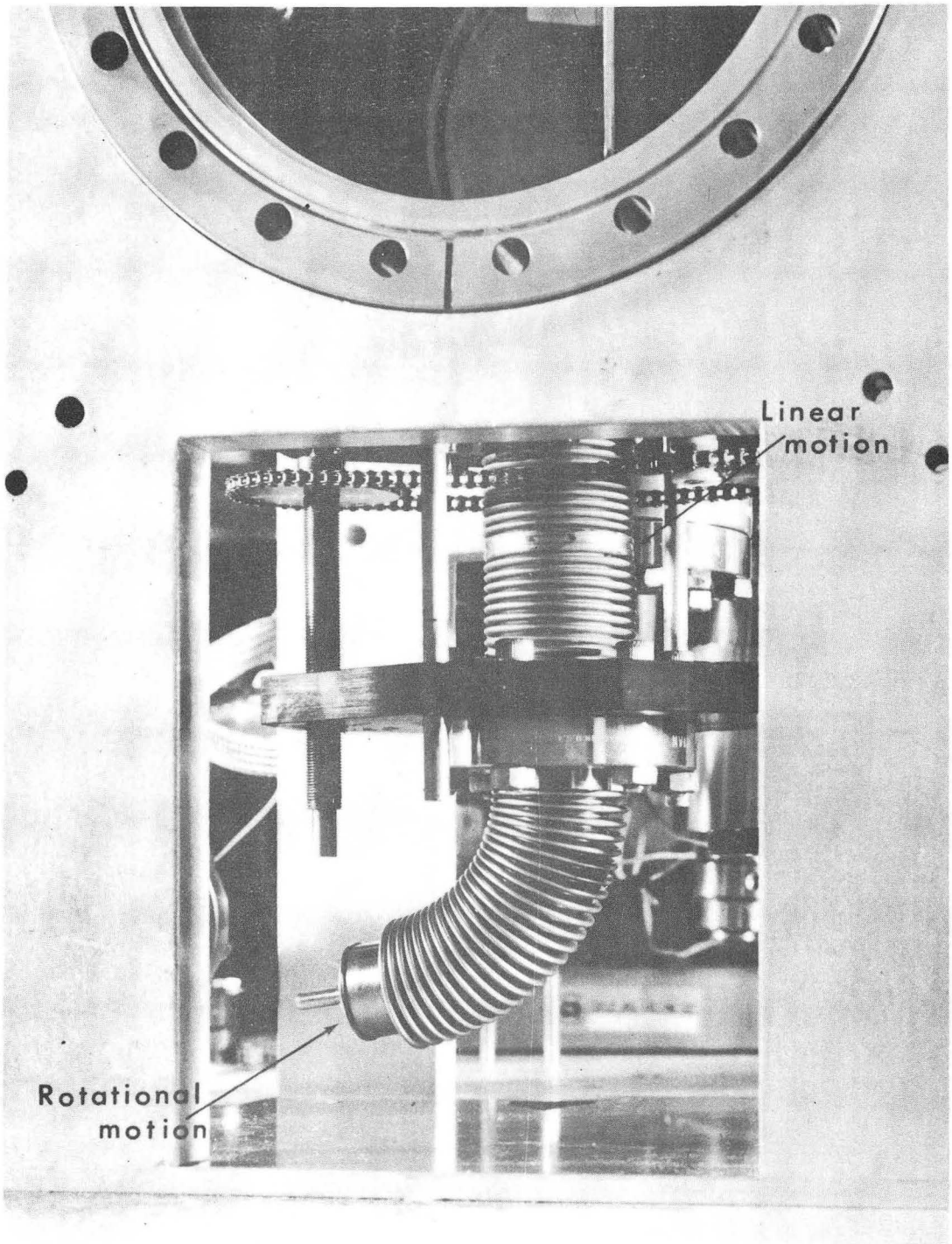

XBB709-3966A

Fig. 10. Rotary motion-linear motion feedthrough.

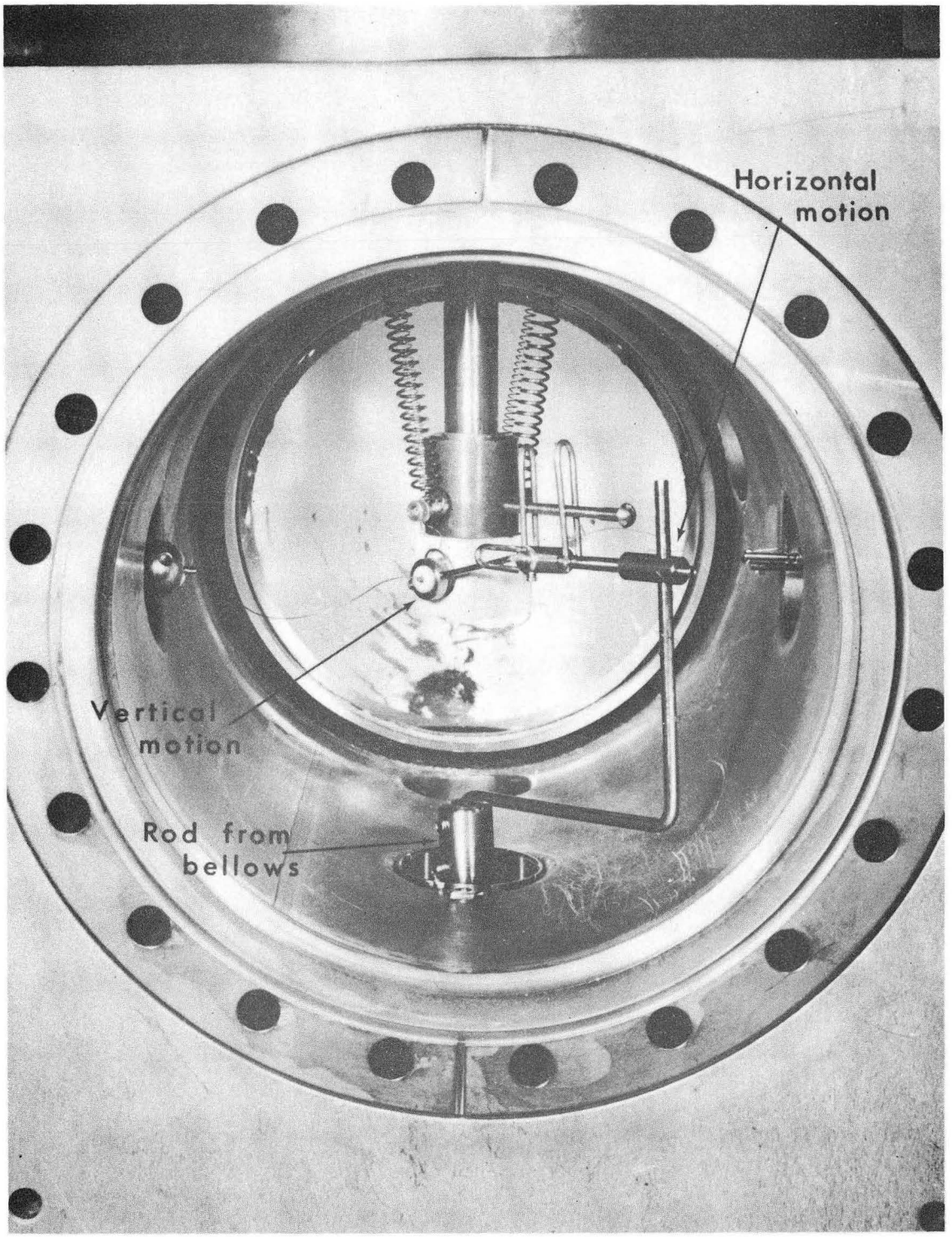

XBB709-3967A

Fig. 11. Mechanism for tip manipulation.

2.4. Instrumentation

The tip voltage is supplied by Sorenson 5010 (1 - 10 kV) and Sorenson 5030 (5 - 30 kV) high voltage sources connected to the same output by a switch. The voltage ripple is guaranteed by the manufacturer to be less than 0.02% of the voltage (rms). As a protective measure the voltage is supplied to the microscope through a large resistor, in connection with which an electrical filter was installed to reduce the ripple further. It is now less than one volt peak-to-peak at all voltage levels, which is negligible for every practical purpose. The voltage is measured with a four place digital volt meter (DVM) over a 1000:1 voltage divider. This set up was calibrated to the accuracy of the DVM which is ±1 digit of the least significant position, i.e. ±10 V at voltages above 10 kV. At present this accuracy is satisfactory.

The field evaporation pulse is provided by a kilovolt nanosecond pulse generator (Microwave Associates, model 961 E). The amplitude of the pulse is variable from 0 to 3000 V, and the pulse width from 2 to 20 nanoseconds. Both rise and fall times are less than a half nanosecond. The pulse height is indicated by a small panel meter, which allows repetition of pulse heights from previous experiments to within ±5%. The voltage supply to the pulse generator is unstabilized. Hence the pulse amplitude will vary with changes in the line voltage. The pulse has an amplitude "jitter" of less than 4% and an overshoot that is less than 10%. All in all the absolute pulse height is not very accurately known. As will be shown later this is not terribly significant, however. The worst shortcoming is the bad repeatability of the pulse height, which is due rather to the pulse height indicator than the generator

itself, and improvements here are easy to effect. The voltage pulse is coupled to the tip through a large capacitor. Due to the ever-present d.c. voltage at the tip the voltage line cannot be terminated and reflections of the pulse will consequently occur. These will increase the effective pulse voltage, and hence make the pulse amplitude even less accurately known. Simultaneously with the high voltage pulse a triggering pulse with an amplitude of about 2% of the high level pulse is generated. This also has a half nanosecond rise time and is used to trigger the timer.

A magnetic electron multiplier (Bendix, M306) is used as ion detector. It produces a pulse with a rise time of less than 5 ns. The transit time through the detector is unspecified but is estimated to be some 50 ns.

The time of flight is recorded with a Tektronic 454 oscilloscope, with a P6045 probe as preamplifier. The delay time through the probe is 11.7 ns, and its rise time less than 1.5 ns, whereas the rise time of the oscilloscope itself is 2-5 ns depending on the deflection factor used. The time is read from the graticule of the oscilloscope screen. The graticule has ten major horizontal divisions, each 0.8 cm wide. Along the center horizontal line each major division is divided into five subdivisions. The reading accuracy can be assessed as about ±0.1 major division. Typical recorded times are in the region 3-10 microseconds so a time base of 1 μs/div is normally used. The reading accuracy is hence ±100 ns. If the time to be measured is approximately known it can be measured more exactly by utilizing the delayed sweep mode of the oscilloscope. For instance a time of flight between 4 and 5 μs can be

measured by delaying the sweep by 4 μs and displaying the next microsecond using 100 ns/div as time base. The reading accuracy would now be ±10 ns, which is about the largest meaningful sensitivity with the present set up. The specified accuracy of the delay time is, only 2-3%, but it can be calibrated by an external oscillator and has turned out to be quite exact and, even more importantly, quite stable over a long period of time. This method can in any case be used to measure the spread of flight times from a tip of a single isotope metal. This would provide a measure of the potential resolving power of the instrument.

3. OPERATION OF THE ATOM-PROBE

For successful operation of the atom probe it is crucial that the tip of the specimen is in alignment with the probe hole and the detector, and that it stays in alignment during operation. To ensure this the specimen is first centered inside the specimen drum in the way illustrated in Fig. 12. A small hole (0.4 mm) is precision drilled through the drum. This hole coincides with the vertical axis of rotation of the specimen holder when the drum is mounted inside the block. A laser beam is passed through the hole and the tip of the specimen is positioned right in the beam by adjusting the depth of the tungsten spring in the copper plug. The weakness of this procedure is that it leaves the position of the tip along the direction of the beam unspecified. This direction is usually checked merely by looking from the front, towards the copper plug, to see that the tip also is positioned on the axis of rotation of the drum itself. This is admittedly a crude method, and is only justified by its evident success. After this centering procedure that positions the tip at the center of rotation of the specimen holder, the laser beam is aligned along the axis of the atom probe as shown in Fig. 13. A small plug with a 0.4 mm hole is inserted in the probe hole to narrow down the beam. The drum with the specimen is mounted on the specimen holder and the tip is adjusted into the beam by tilting the cold finger as explained in connection with Fig. 5. Finally the detector is mounted and centered with the aid of the beam. With this method it is estimated that the tip can be centered to within 0.2 mm of the axis at the probe. That this precision is rather necessary should be obvious from the dimensions of the instrument. The tip-to-screen distance is 12 cm, the detector is 90 cm behind the screen, the diameter of the probe hole is 2 mm, and the

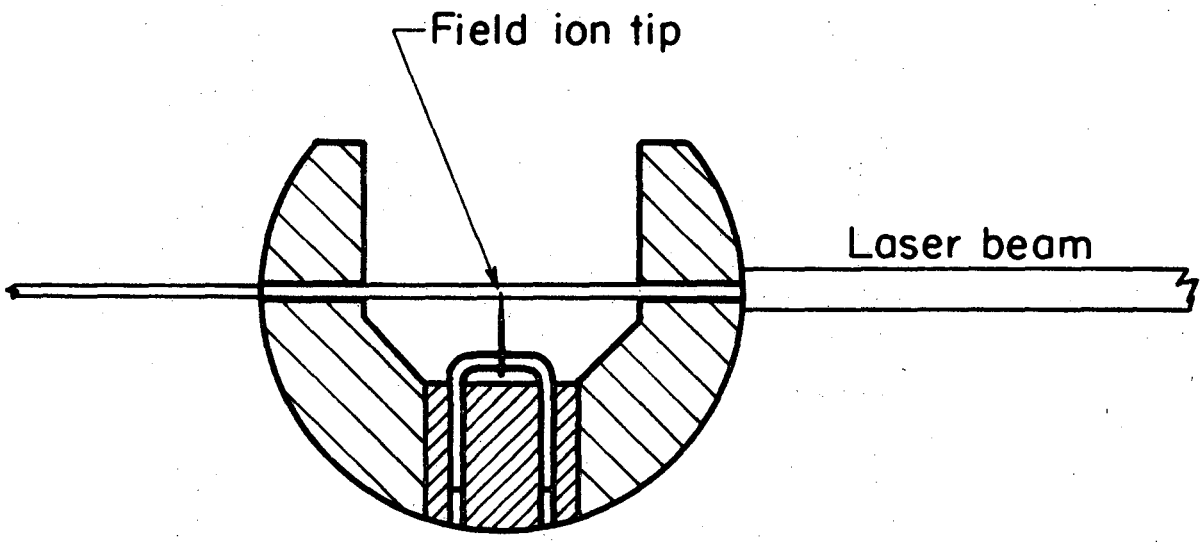

XBL 709-6488

Fig. 12. Centering of the tip in the specimen drum.

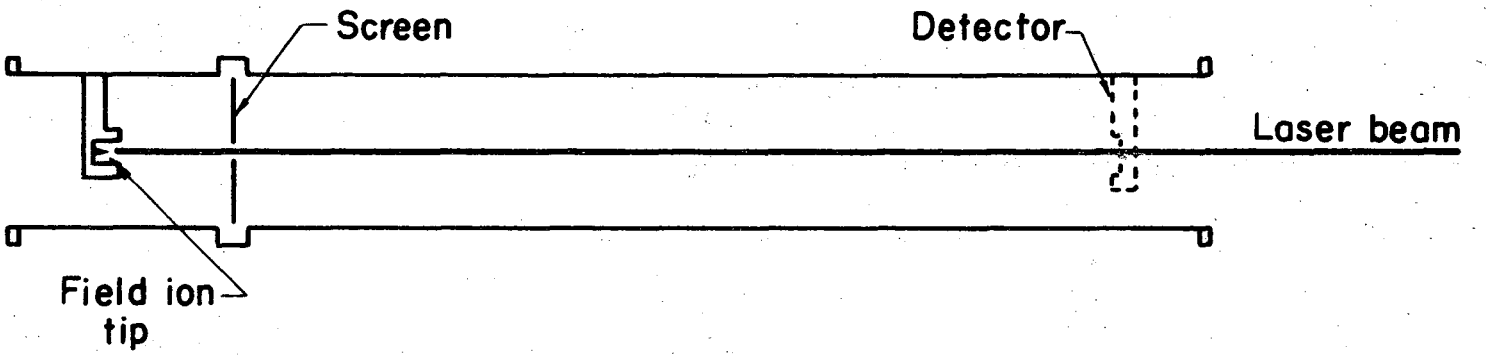

XBL 709-6484

Fig. 13. Alignment of the atom probe.

sensitive area of the detector is 1.6×1.8 cm^2.

Operation of the atom probe involves aiming of the atom chosen for examination into the probe, which in practice means positioning of the image dot over the probe hole in the screen. With the present design and a tip to screen distance of 12 cm the image dots are much smaller than the probe hole (2 mm). In fact, in most parts of the image, two adjacent dots can be accomodated inside the hole. Centering of one particular dot in the probe hole is thus, to some extent, a matter of guesswork but can still be done with fair accuracy. It is highly probable that more than one ion enters the probe hole on the application of an evaporating pulse to the tip. For most applications this makes no difference, however. Müller[1] has observed that at the edge of the (110) plane the hole has to be positioned inside the plane edge in order to get the atom from the edge into the probe. This phenomenon has been confirmed with the present instrument as well. The suggested explanation is that the atom before taking off "rolls" toward the center of the plane. In other regions the probe hole may have to be positioned outside the image dot due to the tangential field component at a kink site that affects the evaporating ion but not the image ions which ionize some 4 Å above the atom.[1] No such effects have been observed, however. At any rate, it is far from obvious that an evaporating ion will follow the same path to the screen as the image ions did. At the present state of the art one cannot even be certain that the detected atom is the same one that was aimed at the probe hole. One should also keep in mind that the evaporation voltage usually is some 10% higher than the image voltage, and that furthermore the evaporation is effected by a voltage

pulse with a duration of only some nanoseconds. Obviously the field conditions are markedly different during pulsed field evaporation and stable imaging. However, an increase of the tip voltage from the best image voltage towards the field evaporation voltage reveals no significant effect on the positions of the image dots, so the higher voltage itself is probably of no concern in this respect. The highly dynamic nature of the field evaporation event may, however, affect the ion path in some unpredicted manner.

Sometimes no ions at all can be detected in the probe despite the fact that the tip is obviously evaporating. In fact, this seemed to be an unsolvable problem when this instrument was first tried. For a period of several months the atom probe simply refused to function, the most careful alignment of the probe and centering of the probe hole on the dots notwithstanding. This behavior remained unexplained when the instrument finally started to work. At present an ion is detected in more than half, and sometimes in 80-90%, of the evaporation events.

4. CALIBRATION AND RESOLUTION OF THE ATOM PROBE

The ultimate goal of mass spectroscopy is, of course, to resolve adjacent atomic masses. For an atomic mass number of 200 this means a relative accuracy of ±0.25%. The maximum relative error in the mass to charge ratio measured according to Eq. (1.3) is

$$\left|\frac{\Delta(m/n)}{m/n}\right| = \left|\frac{\Delta V}{V}\right| + 2\left|\frac{\Delta t_0}{t_0}\right| + 2\left|\frac{\Delta \ell}{\ell}\right| , \qquad (4.1)$$

with $V = V_{dc} + V_{pulse}$. An absolute determination of m/n to the specified accuracy would hence require a measurement of the voltages, time of flight, and length of the flight path to within one part in a thousand. This can be done for the length (1 m ± 1 mm), but as far as the time of flight and the pulse voltage are concerned it is quite impossible with the present system. In view of the data presented in section 2.4 the time recorded on the oscilloscope screen can hardly be trusted to any better than ±5%. Furthermore this time is not the actual time of flight, but contains a sizeable amount of electronic delay as well.

For the voltage pulse the situation is even more complicated. Eq. (1.2) is based on the assumptions that the evaporating ion does not leave the tip before the pulse has reacted its full value and that all of its potential energy is transformed to kinetic energy. The first assumption is quite correct unless the pulse amplitude is very high. For a pulse amplitude that is just enough to evaporate an atom it can be safely stated that the pulse reaches its full value before the atom leaves the tip. Too little is yet known about the kinetics of the field evaporation event to make the same statement with regard to a very large voltage

pulse. It is at least not obvious, however, that the ion could not leave the tip on the rising edge of the pulse and get out of the high voltage region before the pulse reaches its full value. The voltage drops to 1% of its value at the tip in 10^5 - 10^6 Å (0.01 - 0.1 mm) which distance the ion should reach in about 1 ns after take off. Hence with a pulse rise time of 0.5 ns it is conceivable that the ion might "escape" part of the pulse amplitude, in which case it would not receive the total potential energy $V_{dc} + V_{pulse}$ as assumed. It should in this context be kept in mind that the reflection of the pulse may increase its effective value by as much as a factor of 2. The above considerations actually refer to this added pulse. The relevant point to make here is simply that the potential energy of the field evaporated ion is not clearly determined even if the pulse amplitude were accurately known.

The second assumption, that all of the potential energy is transformed to kinetic energy, is not exactly correct, but the error is probably of merely academic interest. The question is whether the ion, while the pulse is still on, will reach a region in space where the difference between the pulse-on and pulse-off potentials is negligible. In 2 ns the ion should travel a distance of about 0.1 - 0.5 mm where the voltage will have dropped by a factor of 10^{-3}. The effect when the pulse falls off should hence be of the order of one volt. For a 20 ns pulse the situation is, of course, even better, and this problem should be of no concern. It should be pointed out here that the use of a longer pulse width does not introduce an uncertainty about the exact time of the field evaporation event since, in all likelihood, the ion leaves the tip within the first nanosecond of the pulse.[10]

Despite the difficulties sketched above the atom probe can be accurately calibrated using the following method.[11] Eq. (1.3) is rewritten in the form

$$\frac{m}{n} = C(V_{dc} + kV_{pulse})\ (t - T)^2 \qquad (4.2)$$

where C is a constant containing the length of the flight path, ℓ, and all the units so that m is in atomic mass units, n in electron charges, the voltages in kV and the times in μs. t is the time measured with the oscilloscope, and thus T represents the delay. The factor k is usually interpreted as the multiplication factor due to the pulse reflection. It is probably more correct to look upon k as a factor that corrects for all the uncertainties in establishing the potential energy of the evaporating ion. V_{dc} is the reading of the digital volt meter that monitors the tip voltage, and V_{pulse} is the setting of the pulse height indicator.

For calibration a single isotope metal for which m/n is exactly known is analyzed in the atom probe. Data, i.e. corresponding values of V_{dc}, V_{pulse}, and t, is collected from the whole possible voltage region (5 - 20 kV). The difference, or actually the square of the difference, between the correct m/n and m/n as calculated from Eq. (4.2) using the data is minimized with respect to k and T, yielding the values of k and T to be used in Eq. (4.2). In mathematical terms a function X is formed:

$$\overline{X} = \Sigma\left\{\left(\frac{m}{n}\right) - C\left(V_{dc_i} + kV_{pulse_i}\right)\left(t_i - T\right)^2\right\}^2, \qquad (4.3)$$

and X is minimized with respect to k and T setting

$$\frac{\partial \overline{X}}{\partial k} = 0$$
$$\frac{\partial \overline{X}}{\partial T} = 0 \qquad (4.4)$$

which equations solved together will yield k and T. A computer program using the Newton-Raphson method has been written out to solve (4.4) numerically. The convergence is very rapid starting for instance with T = 0 and k = 1. Possible one isotope metals to use are ^{9}Be, ^{12}C, ^{27}Al, ^{51}V, ^{59}Co, ^{93}Nb, ^{103}Rh, ^{181}Ta and ^{197}Au.

For the above method to work properly the values of V_{dc} and V_{pulse} must be accurate enough. V_{dc} can as mentioned be measured to within ±10 V. A variation of 10 V at a voltage level of 10 kV means a variation of 0.1% in the mass number according to Eq. (4.1). At present it is believed that the pulse voltage can be set with the same accuracy using a magnifying glass when adjusting the indicator. The pulse voltage generator is evidently the weak point of the instrument, though, and will be improved. With the present accuracy of the time measurement a voltage variation of ±10 V could not be detected in the time of flight. It would correspond to about ±5 ns in t. The calibration method would hence seem to be valid.

Figure 14 shows the result of an attempt to calibrate the atom probe using a tungsten specimen. Tungsten has four isotopes with mass numbers 182, 183, 184 and 186 and thus the method described above could not be applied directly. Instead the raw data (corresponding values of V_{dc}, V_{pulse} and t) was first transformed into m/n values using Eq. (4.2)

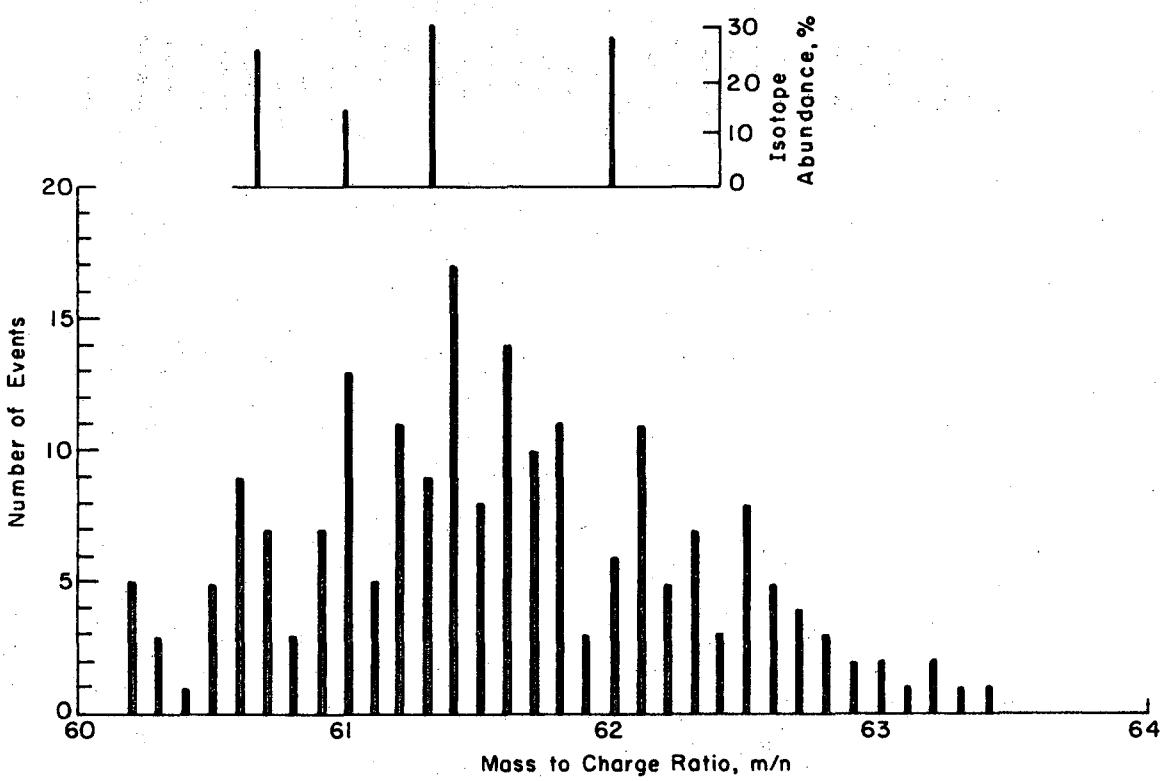

XBL 709-6568

Fig. 14. Mass spectrum of tungsten (W^{+++}).

and estimated values of the constants k and T in order to separate the data corresponding to each isotope. After this a calibration based on the data corresponding to the isotope ^{184}W was carried out yielding the values 1.73 and 0.221 μs for k and T respectively. Using these values for k and T the data was once more transformed into m/n values yielding the result displayed in Fig. 14. Of 276 ions analyzed 1 yielded the value m/n = 54, 57 values between 65.6 and 74, and 222 the values represented in the graph. Only data corresponding to the ion W^{+++} was collected. Tungsten also field evaporates as a quadruply charged ion.

In this particular case the isotopes were not resolved well enough to allow for unambiguous separation of the data, and hence the method used is somewhat questionable. The tip voltage was measured only to within ±10 V at a voltage level between 6.7 and 8.2 kV with a pulse voltage varying from 0.7 to 0.8 kV, also adjusted to within ±10 V. To this must be added the uncertainty of the potential energy of the ion, maybe another ±10 V, and the error of the time of flight ±20 ns, bringing the relative accuracy of the mass analysis to ±0.6% which is not enough to resolve the isotopes of tungsten. Thus the result in Fig. 14, which is one broad peak rather than four separate ones, is no worse than could be expected. The value of the delay time T (221 ns) is about twice as large as expected. This probably depends on a lack of coincidence between the starting point of the oscilloscope sweep and the edge of the graticule on the screen. Since the time of flight is read off the graticule this would add a constant to the time. As long as this "error" stays constant throughout the measurement it does not affect the accuracy of the measurement, and is of no concern. The value of the multiplication constant k(1.73) on the other hand is right in the expected region.

One lesson to be learned from Fig. 14 is the fact that a considerable number of ions must be analyzed before their m/n value can be determined. Analysis of merely one event cannot be trusted.

The extensive number of very large m/n values recorded is somewhat puzzling. This feature has been observed before though, and a suggested explanation is the formation of complexes between the evaporating species and O, H, N, He, etc.[1] Part of these events could also be due to afterpulses in the detector. The event giving the value m/n = 54 is probably a random event caused by a remaining atom of the imaging gas.

To understand how further improvements of the mass resolution of the atom probe could be brought about, an evaluation of the reasons for the broadening of the mass peak is necessary. Especially it is of interest to examine whether an increase of the time of flight can improve the resolution. Relevant conclusions can be drawn directly from Eq. (4.1). The term $|\Delta V/V|$ is independent of t_0 ($t_0 = t-T$) and can only be decreased by measuring the voltages more accurately. With presently available instruments the tip voltage (V_{dc}) could be measured to within one part in 10^5, and the pulse height could be monitored with the four place digital voltmeter with an accuracy of one part in 10^3. This would make $|\Delta V/V|$ negligibly small, save for the possible uncertainty of the potential energy of the ion. In the calibration procedure this error would appear as the statistical variation of the multiplication constant k. In Eq. (4.1) t_0 is to be regarded as a combination of the measurement error of t, Δt, and the spread of the delay time ΔT. If cost were no factor Δt could be made negligible by the use of a digital timer for the time measurement, which could measure the time to within ±1 ns for

any value of t. These improvements in instrumentation would thus leave only ΔT and part of ΔV as significant causes of the line broadening. T is composed of the transit times through the detector and the amplifier, and further of the lack of coincidence between the field evaporation event and the triggering of the timer. The last contribution cannot be larger than a few nanoseconds and hence its variation is negligible. The transit time through the preamplifier is specified as 11.7 ns which indicates that its variation is less than 0.1 ns and hence also negligible. The main contribution to ΔT seems to be the spread of the transit time through the detector. This time itself is some 50 ns and its variation could well be in the 10-20% region, i.e. up to ±10 ns. The significant part of ΔV is, as mentioned, the uncertainty of the energy picked up by the ion from the pulse. Whether ΔV is of comparable magnitude to ΔT is an open question. It should be remembered here that $|\Delta t_0/t_0|$ in Eq. (4.1) is weighted by a factor of two relative to $|\Delta V/V|$. Hence, with a flight time of 10 μs at a voltage of 10 kV, ΔT = 10 ns would be matched by ΔV = 20 V. This seems quite high but not totally implausible. The conclusion to be drawn from this reasoning is, however, that if ΔT dominates the linebroadening an improvement can be effected by increasing the time of flight, but if ΔV dominates it will set a limit on the attainable resolution, to which, at present, no remedies seem to be available.

It is interesting, in this connection, to recall that in the pulsed ring mode of the atom probe mentioned in the introduction, the pulse amplitude does not contribute to the energy of the ion. Hence, if in fact $|\Delta V/V|$ in the case discussed above is significant, the pulsed ring

mode would offer a potentially better resolution. Results reported by Brenner and McKinney[9] for this type of instrument show a very poor resolution however, but this was mainly due to rather poor experimental accuracy. Müller[1] raises very grave criticism against the electrode structure of Brenner's and McKinney's instrument[9] on the ground that, according to him, it will make aiming of a particular surface atom into the probe hole virtually impossible, due to lateral field components when the pulse is applied. Thus it may be that the pulsed ring mode is not usable.

If ΔT and ΔV were of equal importance and of the magnitude assumed above they would limit $\Delta m/m$ to about $\pm 0.4\%$. It should be remembered that the values of both ΔT and ΔV were estimated, probably pessimistically. Thus the value $\pm 0.4\%$ should only be taken as an indication of what can be expected of the instrument. By increasing the time of flight the effect of ΔT can be reduced and the resolution improved even further.

5. THE MODIFIED ATOM PROBE

The analysis of the preceeding section indicated that some improvement of the mass resolution of the atom probe may result from an increase of the time of flight. Of the two methods to accomplish this, increasing the length of the flight path is the more straight forward. It is, for practical reasons, limited to a lengthening of the flight tube by about a factor of two from the present length (1 m), and even doubling the length of the tube will require a focusing device, since the detector is too small to cover the solid angle defined by the tip and the probe hole. The other method of increasing the time of flight, slowing down the ion, is somewhat more complicated to apply, but instead the time of flight can be increased by a factor of ten without increasing the size of the instrument. Focusing will be necessary in this case as well, and this method also suffers from other shortcomings to be discussed below. The atom probe with a device to slow down the ion will be referred to as the modified atom probe.

To be able to analyze the performance of the modified atom probe one must first derive the relationship between the time of flight of the ion and its mass to charge ratio. The geometry of the modified probe is illustrated in Fig. 2, and the design of the focusing lens is described in the appendix. Based on Fig. 2 it would seem natural to divide the time of flight into four parts, and indexing from the left to the right the following expressions are obtained. Flight time from the tip to the lens

$$t_1 = \ell_1 \sqrt{\frac{m}{2qV_0}} \tag{5.1}$$

transit through the focusing lens (see A-15)

$$\tan h \frac{\omega t_2}{\sqrt{2}} = \frac{\ell_2}{\sqrt{V_0}+\sqrt{V_0-V_1}}\sqrt{\frac{c}{q}} \tag{5.2}$$

flight time through the drift tube

$$t_3 = \ell_3\sqrt{\frac{m}{2q(V_0-V_1)}} \tag{5.3}$$

transit through the exit lens

$$t_4 = \ell_4\sqrt{\frac{2m}{q}}\frac{1}{\sqrt{V_0}+\sqrt{V_0-V_1}} \tag{5.4}$$

It should be noticed that all time components except t_2 are of the same form with respect to the mass to charge ratio. The problem is hence how to treat t_2. Some numerical values are compiled in Table 5.1. It is obvious that t_2 is not small enough to be neglected all together, but the difference between t_2 and t_4 (with $l_2 = l_4 = 1.2$ cm) is less than 5% except for very small values of $V_0 - V_1$, where it increases up to 10%. The similarity between t_2 and t_4 is of course to be expected on physical grounds and it can easily be established analytically as well. For the values of the voltages used in Table 5.1 the argument of the hyperbolic tangent in Eq. (5.2) is between 0.2 and 0.3 in which region the hyperbolic tangent may be replaced by its argument with less than 5% error. Doing so Eq. (5.2) reduces to Eq. (5.4) and solving for the mass to charge ratio the following expression results:

$$\frac{m}{n} = C\left\{\frac{t_0}{\frac{\ell_1}{\sqrt{2V_0}}+\frac{\sqrt{2}(\ell_2+\ell_4)}{\sqrt{V_0}+\sqrt{V_0-V_1}}+\frac{\ell_3}{\sqrt{2(V_0-V_1)}}}\right\}^2 \tag{5.5}$$

Table 5.1. The components of the time of flight of the modified atom probe.

V_0/kV	V_1/kV	t_1(15 cm)/μs	t_2/μs	t_3/μs	t_4/μs	t_0/μs	t_1'(100 cm)/μs
5.2	5.0	1.500	.219	40.08	.200	41.999	10.00
5.5	5.0	1.460	.183	25.68	.178	27.501	9.73
6.0	5.0	1.400	.162	18.20	.158	19.920	9.33
7.0	5.0	1.290	.137	12.96	.134	14.521	8.60
10.2	10.0	1.070	.163	40.08	.150	41.463	7.13
10.5	10.0	1.050	.143	25.68	.138	27.011	7.00
11.0	10.0	1.030	.130	18.20	.126	19.486	6.86
12.0	10.0	.990	.115	12.96	.112	14.177	6.60
20.2	20.0	.763	.119	40.08	.141	41.073	5.08
20.5	20.0	.755	.109	25.68	.104	26.648	5.03
21.0	20.0	.745	.101	18.20	.097	19.143	4.96
22.0	20.0	.726	.092	12.96	.089	13.867	4.84
30.2	30.0	.623	.098	40.08	.092	40.893	4.15
30.5	30.0	.620	.091	25.68	.087	26.478	4.13
31.0	30.0	.614	.087	18.20	.083	18.984	4.09
32.0	30.0	.604	.080	12.96	.077	13.721	4.03

The constant C is again introduced for convenience to take care of all the units so that m is expressed in atomic mass units, n in electron charges, t in microseconds, V in kilovolts, and ℓ in centimeters.

Table 5.1 lists the values of the different time components of the modified probe, their sum, and the time of flight in a normal atom probe of the same total length for some typical voltage values. The time t_3 turns out to be more than 90% of the total time in all the listed cases, and is hence overwhelmingly the most important of the time components. As Table 5.1 also shows, t_3 depends only on the voltage difference $V_0 - V_1$, and this difference has to be fairly small, at most 1 kV, if a significant increase of the time of flight is to be achieved. As far as accuracy is concerned this is very unfortunate, since the relative error is much increased when a small difference between two large numbers is formed. It should be remembered in this connection that V_0 stands for $V_{dc} + V_{pulse}$. Hence the uncertainty of V_{pulse} will enter the difference between V_0 and V_1, and its relative significance will be strongly pronounced in the modified atom probe. A ΔV of only 1 V, which is practically negligible in the normal atom probe, would cause a relative error of the order of 0.1% in t_3 with $V_0 - V_1 = 1$ kV. Hence, even if ΔV, the uncertainty in the potential energy of the ion, were overshadowed by ΔT, the spread in the electronic delay, in the normal atom probe, its effect is so much magnified in the modified probe that it becomes dominant, and results in an even poorer resolution.

Again the situation would be more favorable with the pulsed ring mode, since V_0 and V_1 would both be stable dc voltages. Measuring both V_0 and V_1 with an accuracy of one part in 10^5 would still leave

$V_0 - V_1 = 1$ kV specified to within 2-3 parts in 10^4, which is fairly good. Measuring two voltages with such a high accuracy would be rather expensive, however, and would also make performing experiments more cumbersome.

With a fairly large difference between V_0 and V_1 the accuracy would not suffer significantly and used in this manner the lens system could be used to shorten the flight tube to, say, 40-50 cm, which would save some space and, maybe, reduce the pumping time.

As it stands Eq. (5.5) is far more complicated than Eq. (4.2). As a first approximation the terms containing ℓ_1 and $\ell_2+\ell_4$ could be neglected in the denominator giving Eq. (5.5) the same form as Eq. (4.2). A calibration with two adjustable constants would not apply in this case, however, since the error of the approximation is voltage dependent. Thus more involved calibration methods would have to be devised for the modified atom probe.

Thus the modification of the atom probe would only make the use of the instrument more complicated,without offering any essential improvements. At the time being there seems to be no reason to pursue the modified probe any further. In its present condition the atom probe performs excellently and its mass resolution is sufficient for many applications. If better resolution is required the way to achieve that would be, as a first step, to improve the instrumentation, and, possibly, as a second step, to increase the length of the flight tube.

ACKNOWLEDGEMENTS

The author wishes to put on record his great indebtedness to Dr. Hua-Ching Tong. The patient support of his supervisor Prof. Jack Washburn is also gratefully acknowledged. This work was done under the auspices of the U. S. Atomic Energy Commission.

APPENDIX. A FOCUSING ION LENS

The purpose of the lens is to focus the entering ions onto the exit aperture of the drift tube, or essentially on the detector. Since the detector is fairly large the focusing requirement is not very stringent. Figure 2 shows the geometry of the device. The focusing electric field is created in the space between z = 0 and z = a.

A focusing field is specified by requiring that the field exert an elastic radial force towards the axis on the ion of the form[12]

$$F_r = -cr, \tag{A1}$$

where c is a constant. We have further

$$F_r = -q\frac{\partial V}{\partial r}, \tag{A2}$$

where q is the charge of the ion and V is the potential. With the aid of these equations Laplace's equation in cylindrical coordinates,

$$\frac{\partial^2 V}{\partial r^2} + \frac{1}{r}\frac{\partial V}{\partial r} + \frac{\partial^2 V}{\partial z^2} = 0, \tag{A3}$$

can be solved yielding

$$V = V_m - \frac{c}{q}(z - Z_m)^2 + \frac{c}{2q}r^2. \tag{A4}$$

The constants V_m and c/q can be determined from the boundary conditions

$$\begin{cases} V(r=0,\ z=0) = 0 \\ V(r=0,\ z=a) = V_1 . \end{cases} \tag{A5}$$

Thus V_m and c/q become

$$V_m = \frac{V_1 Z_m^2}{a(2Z_m - a)} \quad , \quad \frac{c}{q} = \frac{V_1}{a(2Z_m - a)} \; . \tag{A6}$$

Z_m and a remain as parameters of the potential.

Writing Eq. (A4) in the form

$$\frac{(z-Z_m)^2}{\frac{q}{c}(V_m - V)} - \frac{r^2}{\frac{2q}{c}(V_m - V)} = 1 \tag{A7}$$

reveals that the equipotential surfaces are hyperboloids of rotation with asymptotes

$$r_{1,2} = \pm \sqrt{2}\,(z - Z_m) \; . \tag{A8}$$

Especially the equipotentials at V = 0, and V = V_1 are:

$$\begin{cases} V=0, & \dfrac{(z-Z_m)^2}{Z_m^2} - \dfrac{r^2}{2Z_m^2} = 1 \\ V=V_1, & \dfrac{(z-Z_m)^2}{(Z_m-a)^2} - \dfrac{r^2}{2(Z_m-a)^2} = 1 \end{cases} \tag{A9}$$

The lens is constructed by fabricating two surfaces according to Eq. (A9) and supporting them at the proper distance from one another.

To determine suitable values for Z_m and a, the trajectory of an ion through the lens and drift tube is calculated. The equations of motion of an ion in a cylinder symmetric field read

$$\begin{cases} m\ddot{r} = -q\dfrac{\partial V}{\partial r} \\ m\ddot{z} = -q\dfrac{\partial V}{\partial z} \end{cases} \tag{A10}$$

From this one obtains the following equations in the field Eq. (A4):

$$\begin{cases} \ddot{r} = - s \frac{c}{q} r \\ \ddot{z} = s \frac{2c}{q} (z-Z_m) \end{cases} \tag{A11}$$

where s = q/m is the charge to mass ratio of the ion. Equations (A11) have the solution:

$$\begin{cases} r = r_0 \cos \omega t + \frac{\dot{r}_0}{\omega} \sin \omega t \\ z = \frac{\dot{z}_0}{\sqrt{2}\,\omega} \sin h\{\sqrt{2}\,\omega t\} + Z_m(1-\cos h\{\sqrt{2}\,\omega t\}) \end{cases} \tag{A12}$$

where $\omega = \frac{sc}{q}$, and the boundary conditions

$$\text{at } t=0 \quad \begin{cases} r=r_0, \ \dot{r}=\dot{r}_0 \\ z=0 \ , \ \dot{z}=\dot{z}_0 \end{cases} \tag{A13}$$

have been used. The transit time through the lens, T, can be solved from Eq. (A12) if one notices that

$$\begin{aligned} z(T) &= a \\ \dot{z}(T) &= \sqrt{2s(V_0-V_1)} \end{aligned} \tag{A14}$$

After some manipulation the result emerges as

$$\tan h \left\{\frac{\omega T}{\sqrt{2}}\right\} = \frac{a}{Z_m \sqrt{V_0/V_m} + \sqrt{(V_0-V_1)/V_m}} \tag{A15}$$

Computer calculations showed that with Z_m = 46 mm and a = 12 mm the radial distance of the ions from the axis at the exit of the drift tube was less than 5 mm for values of V_0-V_1 ranging from 50 V to 400 V and of V_0 from 5 kV to 30 kV. In these calculations the ions entered the lens at 0.5 mm from the axis with a charge to mass ratio of 1 electron charge/100 amu.

REFERENCES

1. E. W. Müller and T. T. Tsong, Field Ion Microscopy, Principles and Applications, American Elsevier Publishing Co., Inc., New York 1969.

2. E. W. Müller, Z. Physik 106, 541 (1937).

3. E. W. Müller, Z. Physik 120, 270 (1943).

4. E. W. Müller, Z. Physik 131, 136 (1951).

5. E. W. Müller, J. Appl. Phys. 27, 474 (1956).

6. E. W. Müller, J. Appl. Phys. 28, 1 (1957).

7. E. W. Müller, Phys. Rev. 102, 618 (1956).

8. E. W. Müller, J. A. Panitz, S. B. McLane, Rev. Sci. Instr. 39, 83 (1968).

9. S. S. Brenner, J. T. McKinney, Appl. Phys. Letters, 13, 29(1968).

10. E. W. Müller, S. B. McLane, S. V. Krishnaswamy, 17th Field Emission Symposium, Yale Univ., Aug. 1970.

11. J. A. Panitz, S. B. McLane, E. W. Müller, Rev. Sci. Instr. 40, 1321 (1969).

12. K. Schlesinger, IRE Trans on Electron Devices, 8, 224 (1961).

TECHNICAL INFORMATION DIVISION
LAWRENCE RADIATION LABORATORY
UNIVERSITY OF CALIFORNIA
BERKELEY, CALIFORNIA 94720